Measurement of Forces due to Sputtering of Solid Surfaces

IEPC-2015-236／ISTS-2015-b-236

Presented at Joint Conference of 30th International Symposium on Space Technology and Science,
34th International Electric Propulsion Conference and 6th Nano-satellite Symposium
Hyogo-Kobe, Japan
July 4–10, 2015

Alexander Spethmann* , Thomas Trottenberg†, and Holger Kersten‡
Institute of Experimental and Applied Physics, University of Kiel, 24098 Kiel, Germany

This paper reports on first angle- and energy-dependent measurements of forces related to sputtering of solid surfaces carried out with our new realization of a force measuring probe. The force probe measures interferometrically the two-dimensional vector of the forces acting on a measurement target of 20 mm diameter. The measurements have been performed in our ion beam experiment based on a three-grid electron cyclotron resonance ion source. Inside a 530-liter test chamber, a turnable platform carries the force probe and enables to change the angle of incidence of the ion beam at the target. The experimental results are compared with simulations based on the SRIM code.

Nomenclature

U_{anode}	= anode voltage of the ion source
U_{grid}	= middle (accelerator) grid potential of the ion source
U_{pp1}	= plasma potential in the ion source (measured relative to the anode)
U_{pp2}	= plasma potential in the vacuum chamber (measured relative to the walls)
E_{ion}	= beam ion energy
m_{Ar}	= mass of an argon atom
$\vec{n}$	= (inwards directed) target normal
F_1	= component of the force measured by the first displacement sensor
F_2	= component of the force measured by the second displacement sensor
$\vec{F}$	= force vector acting on the target of the force probe
F_{normal}	= component of the force vector normal to the target surface
$F_{\mathrm{in-plane}}$	= component of the force vector in the plane of the target surface
$\vec{p}$	= momentum transferred to the target of the force probe
$\vec{p}_{\mathrm{in}}$	= momentum of impinging beam particles
$\vec{p}_{\mathrm{out}}$	= momentum of released particles
p_{normal}	= component of the momentum vector normal to the target surface
$p_{\mathrm{in-plane}}$	= component of the momentum vector in the plane of the target surface
α	= angle between (inwards directed) target normal $\vec{n}$ and the beam axis $\vec{a}$, also tilt angle or incident angle of beam particles
β	= angle between the force vector $\vec{F}$ and the (inwards directed) target normal $\vec{n}$

*PhD student, Plasma Technology, spethmann@physik.uni-kiel.de
†Research Associate, Plasma Technology, trottenberg@physik.uni-kiel.de
‡Professor, Plasma Technology, kersten@physik.uni-kiel.de

I. Introduction

ENERGETIC particles, i.e. ions or neutrals, colliding with a solid body initiate collision cascades in whose course energy and momentum are transferred to the body. Either the cascades remain in the solid or one or more branches come back to the surface. If the energy of a near-surface particle is still higher than the surface binding energy, the particle leaves the surface into the surrounding vacuum. These sputtered particles may deposit on surfaces of neighboring solid state bodies. The sputter process depends on energy, mass and angle of incidence of the bombarding particles as well as on the material properties of the target (in particular atomic mass, surface binding energy and crystal orientation).

In case of spacecraft surfaces, sputtering leads to erosion of the thruster and modification of the spacecraft surfaces. For instance, beam optics can be changed due to sputtering of the thruster grid system. Also sputtered particles may be deposited on solar cell arrays and change their efficiency. Therefore, sputtering data is a valuable contribution for optimizing a spacecraft design with regard to lifetime and efficiency.

The sputtering effect is commonly quantified by the sputtering yield, i.e. sputtered particles per incident particles. The experimental determination of sputtering yields is commonly done by measurements of mass changes, thickness changes, detection of sputtered particles with spectroscopic techniques and the accumulation of sputtered materials on collectors. Arrangements of a few collectors in the sputter target plume enable emergent-angle-dependent measurements. However, all these techniques do not allow angle-dependent measurements of energies in the sputter target plumes. Energy resolved mass spectrometry may allow for energy dependent measurements, however, such measurements usually do not include a variation of the emergent-angle for practical reasons.

In this contribution, we present angle- and energy-dependent measurements in the beam of an ion source. The targets are part of a novel force measuring probe.[1] The diagnostic is operated in the beam of a three-grid ion source based on electron cyclotron resonance.[2] The forces result both from the impinging energetic beam particles (ions and neutrals) and from the sputtered and reflected particles. The measurements are compared with simulations based on the popular SRIM code.[3] SRIM computes the angle and energy distribution of sputtered and reflected particles applying the binary collision approximation.

II. Experimental Setup

A. Ion Beam Environment

The measurements of forces on a target of copper with the new force probe are performed in our HIBEX *(horizontal ion beam experiment)* chamber (Fig. 1). The ion beam is generated by a three-grid broad beam ion source which differs from the ones described in Ref. 2 only in the grid system. In the source, an argon plasma is produced by means of microwaves and electron cyclotron resonance. Permanent magnets provide the magnetic field, and an antenna emits approximately 360 W of 2.4 GHz microwaves through a quartz cup into the source chamber. Three spherically curved molybdenum grids with a curvature radius of 300 mm extract, accelerate and focus the ion beam. The inner (screen) grid is floating, the middle (accelerator) grid potential is $U_{\text{grid}} = -300\,\text{V}$ and the outer (decelerator) grid is grounded throughout this paper. An anode ring in the ceramic source chamber allows to shift the potential of the source plasma by means of the voltage $U_{\text{anode}} = +(0\dots1200)\,\text{V}$ to corresponding positive potentials $U_{\text{anode}} + U_{\text{pp1}}$, where U_{pp1} is the potential difference between the plasma in the source chamber and the anode due to the plasma sheath at the anode. Measurements with cylindrical Langmuir probes inserted through the grid holes revealed a potential drop of $U_{\text{pp1}} = +(60 \pm 10)\,\text{V}$.

The vacuum chamber is basically a stainless steel cylinder with an inner diameter of 65 cm and a length of 160 cm. The argon pressure in the target chamber is $p_{\text{gas}} = 2 \times 10^{-2}\,\text{Pa}$. The ion beam leaves the source at one end of the vacuum chamber, passes the chamber horizontally above the radially and axially movable carriage unit with the measurement platform, and ends after a length of approximately 140 cm at the opposed beam dump.

The plasma potential U_{pp2} in the vacuum chamber was measured for an anode potential of $U_{\text{anode}} = 1200\,\text{V}$ at all accessible radial and axial positions with an emissive probe and is found to be in the range of $U_{\text{pp2}} = +(40 \pm 10)\,\text{V}$. This measurement allows a calculation of the energy of the beam ions $E_{\text{ion}} = e(U_{\text{anode}} + U_{\text{pp1}} - U_{\text{pp2}})$ from the potential drop between the source and target plasmas.

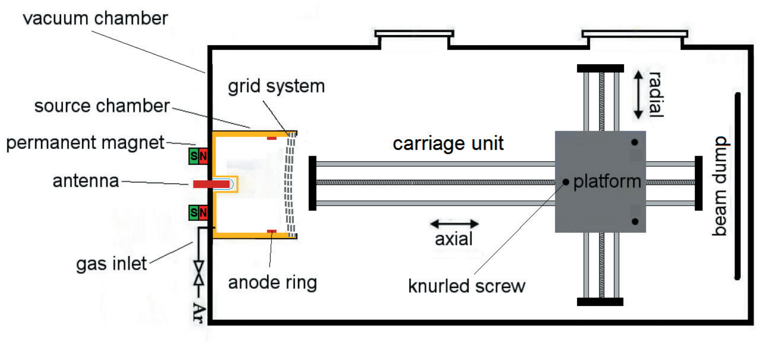

Figure 1. Schematic plan view of the cylindrical HIBEX chamber with the broad beam ion source. The measurement platform is mounted on the carriage unit. (For better visibility, the parts are not true to scale.)

B. Rotatable Force measuring probe

The force probe (Fig. 2) is composed of the measurement target, which is fixed at a ceramic tube that acts as a cantilever beam. The cantilever beam is fixed at the end opposite to the target. Two orthogonally orientated interferometric displacement sensor optics are directed toward two orthogonally orientated mirrors fixed at the beam. Forces acting on the target lead to a bending of the cantilever beam and a displacement of the target mainly in the plane orthogonal to the cantilever beam spanned by the directions of F_1 and F_2. The deflection of the cantilever beam leads to extension or shortening of the laser beam path between the interferometric displacement sensors and the respective mirrors. More details regarding the force probe's setup and its calibration are subject of a companion paper in this conference proceedings[1].

The force probe is mounted vertically with its cantilever on a horizontal turnable platform driven by a stepper motor. The force probe's cantilever beam is arranged in the prolongation of the vertical rotational axis of the turnable platform. The force probe's target surface is placed at the symmetry axis of the ion beam source. The tilt angle of $\alpha = 0°$ is defined for parallel orientation of the (inwards directed) target normal $\vec{n}$ and the ion beam axis $\vec{a}$. Varying the tilt angle enables to measure at different angles of incidence.

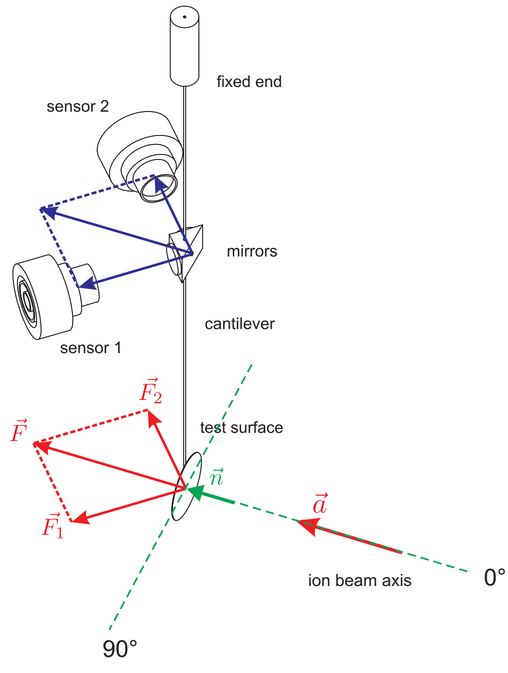

Figure 2. Essential parts of the interferometric force probe and its adjustable orientation relative to the ion beam.

III. Measurements of the force vector

In the following, measurements of forces acting on the force probe's measurement target are presented. The target is positioned at an axial distance of 880 mm on the symmetry axis of the ion source. The measurements have been performed for variable angles of incidence and beam energies. Finally, the measurements are compared with numerical simulations.

A. Angle-dependent force measurements and simulations

The force on the target is composed of incident beam particles (Ar^+ and, due to charge-exchange collisions, Ar), sputtered target particles and reflected beam particles. The two displacement sensors of the force probe measure two linearly independent components of the resulting force vector (see Fig. 2).

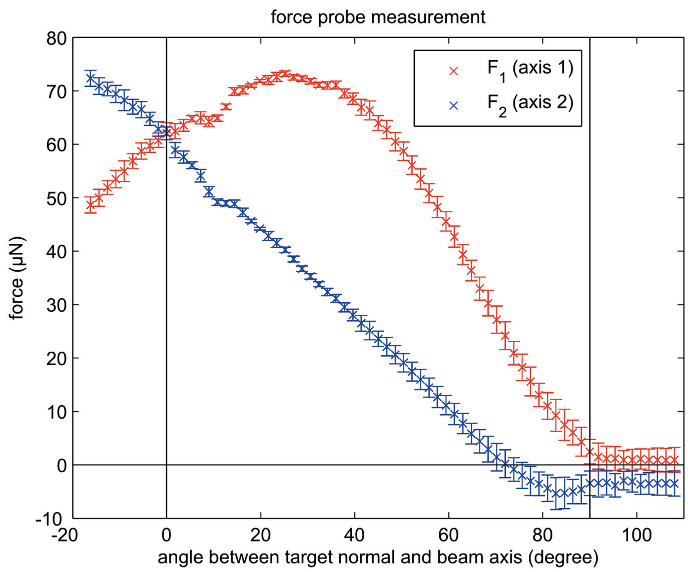

Figure 3. Angle-dependent measurements of forces acting on the force probe's target with the two interferometric sensors at $U_{anode} = 1200$ V.

In Fig. 3, the two force components are plotted over the angle between (inwards directed) target normal $\vec{n}$ and beam axis $\vec{a}$, i.e. the angle of incidence. The blue markers show an almost linear decrease of forces that can be explained geometrically by turning the second sensor (see Fig. 2) away from the beam axis. The red markers show an increase of forces up to about $(45/2)°$ by turning the first sensor into the beam axis. Thereafter, turning the sensor further leads to decreasing forces. The red and the blue profiles intersect at an angle of incidence of $\alpha = 0°$, which shows that the alignment of force probe, turning unit and ion source is well adjusted. Because of the symmetric arrangement of both sensors about the target, the blue profile mirrored at the 0°-vertical matches with the red profile.

The force vector $\vec{F}$ is caused by all impinging beam particles, reflected beam particles and sputtered particles leaving the target. The force probe measures the projections of the force vector onto its two axes providing F_1 and F_2 (see Fig. 2). Due to their perpendicular arrangement, the force vector's magnitude is $|\vec{F}| = \sqrt{F_1^2 + F_2^2}$. The angle β between the force vector and the (inwards directed) target normal can be determined geometrically. In Fig. 4 (a), the force vector's magnitude is plotted over its angle to the (inwards directed) target normal, while in Fig. 4 (b), the angle of the force is plotted over the angle of incidence. The deviation of the curve plotted in Fig. 4 (b) from the diagonal with slope 1 can be attributed to the repulsion of the sputtered target atoms and reflected beam particles.

The force components normal to the target surface and in its plane are projections of the force vector, i.e. $F_{\text{normal}} = |\vec{F}| \cos\beta$ and $F_{\text{in-plane}} = |\vec{F}| \sin\beta$. Fig. 5 (a) shows the normal force plotted over the angle of incidence. The decrease of normal forces at higher angles up to 90° is in part due to the decreasing effective target surface ("$\cos\alpha$ effect"), but also due to the increasing angle β between the force vector and the (inwards directed) target normal ("$\cos\beta$ effect"). Fig. 5 (a) also shows the in-plane force, i.e. parallel to the surface, plotted over the angle of incidence. Up to approximately $\alpha = 45°$, the in-plane force increases because the momentum of the incident particles has an increasing component in the plane of the target. At angles higher than $\alpha = 45°$, the decrease of the effective target surface ("$\cos\alpha$ effect") predominates and leads to a decrease of the measured in-plane force. Additionally, the outgoing particles cause a repulsion in the opposite direction.

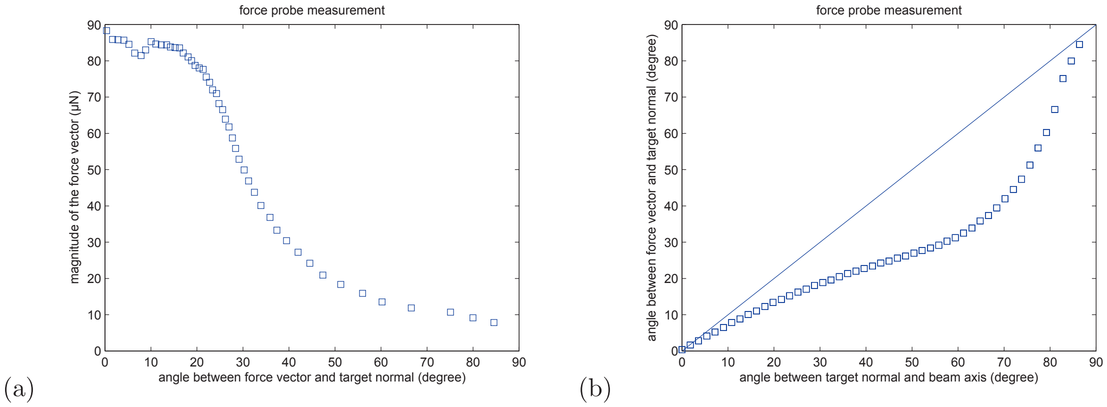

Figure 4. (a) Magnitude of the force vector plotted over its angle to the (inwards directed) target normal. (b) Angle between force vector and (inwards directed) target normal over the angle of incidence.

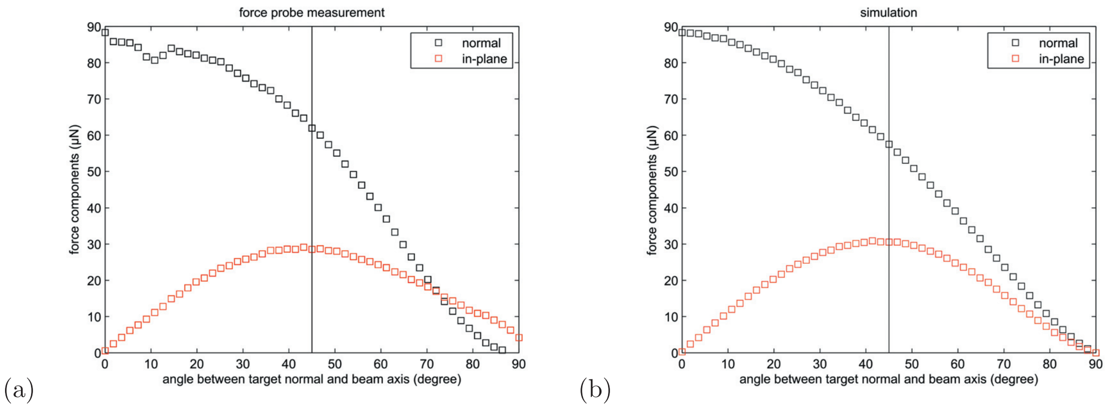

Figure 5. (a) Measurement and (b) simulation of the force normal and parallel to the target surface.

Fig. 5 (b) shows the result of the simulations with the SRIM code for the calculation of two-body atomic collision cascades. For each incident angle between $\alpha = 0°$ and $90°$, 10 000 ion impacts with an energy of $E_{\text{ion}} = 1220\,\text{eV}$ are calculated. For each angle of incidence, the momenta of the from the surface released particles are summed ($\vec{p}_{\text{out}}$). The momentum transfer from the impinging beam particles is considered with $|\vec{p}_{\text{in}}| = 10\,000\,\sqrt{2\,m_{\text{Ar}}\,E_{\text{ion}}}$, where m_{Ar} is the mass of an argon ion or atom. The resulting vectorial momentum $\vec{p} = \vec{p}_{\text{in}} - \vec{p}_{\text{out}}$ is projected onto the target plane and the target's normal in order to obtain the components $p_{\text{in-plane}}$ and p_{normal}, respectively. The forces in arbitrary units are then $\vec{F}_{\text{in-plane}} \propto \vec{p}_{\text{in-plane}} \cos\alpha$ and $\vec{F}_{\text{normal}} \propto \vec{p}_{\text{normal}} \cos\alpha$, where the cosine-factors take the change of effective surface into account. Each force vector of the simulations was scaled by the force value of the measurements at $\alpha = 0°$, and therefore, the normal force values at 0° are equal. Essentially, the simulations are consistent to the measurements.

B. Energy-dependent force measurements and simulations

In Fig. 6, the normal components of the (a) measured and (b) simulated forces are plotted over the tilt angle. In Fig. 7, the in-plane forces are plotted. Again, the simulated force vectors were scaled by the measurements at $\alpha = 0°$. Essentially the simulations are consistent to the measurements for all energies.

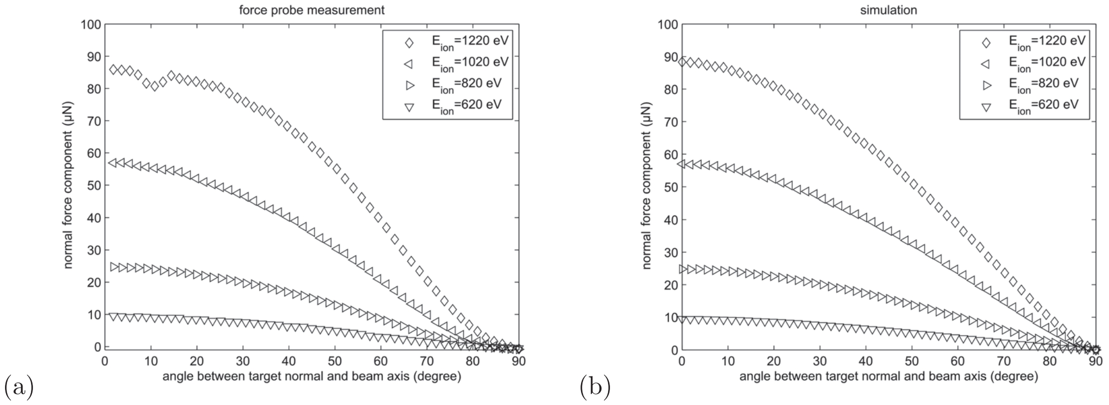

Figure 6. Energy-dependent (a) measurements and (b) simulations of the force normal to the target surface for beam energies between 620 eV and 1220 eV.

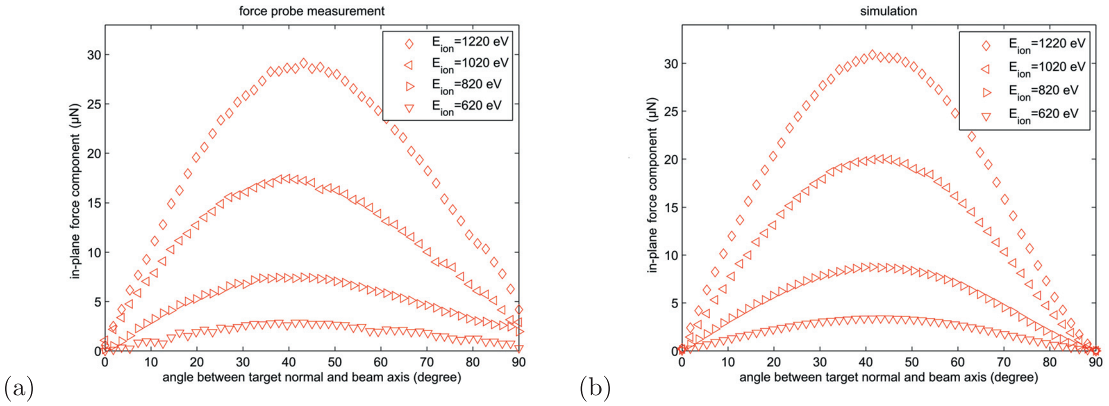

Figure 7. Energy-dependent (a) measurements and (b) simulations of the force parallel to the plane of to the target surface for beam energies between 620 eV and 1220 eV.

IV. Conclusion

In this contribution, angle- and energy-dependent measurements of forces on a target in an ion beam with a novel interferometric force measuring probe have been presented. The ability to measure forces in the plane perpendicular to the target's surface allows for the first time to determine the force vector acting on the target in two dimensions. The force components normal to the target's surface and in its plane are obtained by the projection of the force vector. The measurements are found to be consistent with simulations of two-body atomic collision cascades calculated with the SRIM code for all the measurements with beam energies from E_{ion} =0.6 keV to 1.2 keV.

Acknowledgments

This work is supported by the German Aerospace Center DLR, Project No. 50 RS 1301.

References

[1]Trottenberg, T., Spethmann, A., and Kersten, H., "An Interferometric Force Probe for Thruster Plume Diagnostics," *34th International Electric Propulsion Conference, Kobe, Japan*, 2015, pp. IEPC–2015–419.

[2]Zeuner, M., Scholze, F., Neumann, H., Chass, T., Otto, G., Roth, D., Hellmich, A., and Ocker, B., "A unique ECR broad beam source for thin film processing," *Surf. Coat. Technol.*, Vol. 142–144, 2001, pp. 11–20.

[3]Ziegler, J. F., Biersack, J. P., and Ziegler, M. D., *SRIM – The Stopping and Range of Ions in Matter*, SRIM Co., Chester, Maryland, 2008.